

Electronic Supplementary Information

Experimental section

Materials: Chromium acetate ($C_6H_9O_6Cr$), polyacrylonitrile (PAN), and dimethylformamide (DMF) were purchased from Aladdin Ltd. (Shanghai, China). All reagents were analytical reagent grade and used as received without further purification. The water used throughout all experiments was purified through a Millipore system.

Preparation of Cr_2O_3 nanofibers: 1.0 g PAN was dissolved in 13 mL DMF solution with stirring to obtain a homogeneous solution. Then 1.5 g $C_6H_9O_6Cr$ was added to above solution with gentle stirring for 24 h. A viscous solution can be obtained after gentle stirring for 24 h. Subsequently, the precursor solution was loaded into a plastic syringe for electrospinning by applying a high voltage of 20 kV and the aluminum foil collector with a distance of 15 cm. Next, the obtained precursor nanofibers were calcinated at 230 °C for 1 h with a heating rate of 1 °C min^{-1} and then at 600 °C for 2 h with a heating rate of 2 °C min^{-1} in air. The obtained Cr_2O_3 nanofibers were washed with water for several times and collected by centrifugation, followed by drying at 60 °C.

Preparation of Cr_2O_3 /CPE: 4 mg Cr_2O_3 and 10 μL of Nafion solution (5 wt%) were dispersed in 990 μL mixed solution contain 490 μL ethanol and 500 μL H_2O by 1 h sonication to form a homogeneous ink. Then 25 μL catalyst ink was loaded on a CPE with area of 1 x 1 cm^2 and dried under ambient condition.

Characterizations: XRD data were recorded using a LabX XRD-6100 X-ray diffractometer, with a Cu $K\alpha$ radiation (40 kV, 30 mA) of wavelength 0.154 nm (SHIMADZU, Japan). SEM images were obtained on a Hitachi S-4800 field emission scanning electron microscope at an accelerating voltage of 20 kV. TEM characterization was performed using a HITACHI H-8100 electron microscopy (Hitachi, Tokyo, Japan) operated at 200 kV. XPS data were acquired on an ESCALABMK II X-ray photoelectron spectrometer using Mg as the exciting

source. UV-Vis spectra were acquired on a SHIMADZU UV-1800 ultraviolet-visible spectrophotometer. The ion chromatography data were collected on Swiss Wangtong ECO.

Electrocatalytic N₂ reduction measurements: The N₂ reduction experiments were carried out in a two-compartment cell separated by a Nafion 211 membrane under ambient condition using a CHI 660E electrochemical analyzer. The membrane was protonated by first boiling in ultrapure water for 1 h and treating in H₂O₂ (5%) aqueous solution at 80 °C for another 1 h, respectively. And then, the membrane was treated in 0.5 M H₂SO₄ for 3 h at 80 °C and finally in water for 6 h. The electrochemical experiments using a three-electrode configuration with prepared electrodes, graphite rod and Ag/AgCl electrode (saturated KCl electrolyte) as working electrode, counter electrode and reference electrode, respectively. The potentials reported in this work were converted to reversible hydrogen electrode (RHE) scale via calibration with the following equation: $E \text{ (vs. RHE)} = E \text{ (vs. Ag/AgCl)} + 0.256 \text{ V}$ and the presented current density was normalized to the geometric surface area. For electrochemical N₂ reduction, chrono-amperometry tests were conducted in N₂-saturated 0.1 M HCl solution. All NRR experiments were carried out at room temperature and atmospheric pressure. Prior to each test, the electrolyte was bubbled with Ar or N₂ for 30 min.

Determination of NH₃: Concentration of produced NH₃ was spectrophotometrically determined by the indophenol blue method.¹ Typically, 2 mL HCl electrolyte was taken from the cathodic chamber, and then 2 mL of 1 M NaOH solution containing 5% salicylic acid and 5% sodium citrate was added into this solution. Subsequently, 1 mL of 0.05 M NaClO and 0.2 mL of 1% C₅FeN₆Na₂O·2H₂O were added into the above solution. After standing at room temperature for 2 h, the UV-Vis absorption spectrum was measured at a wavelength of 655 nm. The concentration-absorbance curves were calibrated using standard NH₄Cl solution with a series of concentrations. The fitting curve ($y = 0.370x + 0.076$, $R^2 = 0.999$) shows good linear relation of absorbance value with NH₄Cl concentration by three times independent calibrations.

Determination of N₂H₄: The N₂H₄ presented in the electrolyte was estimated by the method of Watt and Chrisp.² A mixed solution of 5.99 g C₉H₁₁NO, 30 mL HCl and 300 mL ethanol was used as a color reagent. Calibration curve was plotted as follow: first, preparing a series of reference solutions; second, adding 5 mL above prepared color reagent and stirring 20 min at room temperature; finally, the absorbance of the resulting solution was measured at 455 nm, and the yields of N₂H₄ were estimated from a standard curve using 5 mL residual electrolyte and 5 mL color reagent. Absolute calibration of this method was achieved using N₂H₄·H₂O solutions of known concentration as standards, and the fitting curve shows good linear relation of absorbance with N₂H₄·H₂O concentration ($y = 1.01x + 0.045$, $R^2 = 0.998$) by three times independent calibrations.

Determination of FE: The FE for N₂ reduction was defined as the amount of electric charge used for synthesizing NH₃ divided the total charge passed through the electrodes during the electrolysis. The total amount of NH₃ produced was measured using colorimetric methods. Assuming three electrons were needed to produce one NH₃ molecule, the FE could be calculated as follows:

$$FE = 3 \times F \times [NH_3] \times V / 17 \times Q$$

The rate of NH₃ formation was calculated using the following equation:

$$v_{NH_3} = [NH_3] \times V / t \times m_{cat}$$

Where F is the Faraday constant, [NH₃] is the measured NH₃ concentration, V is the volume of the HCl electrolyte for NH₃ collection, t is the reduction time and m_{cat} is the catalyst loading mass.

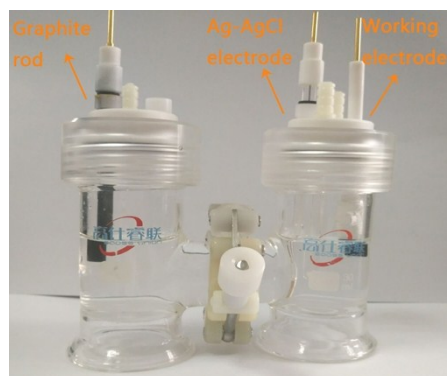


Fig. S1. The construction of two-compartment cell with three-electrode cell and the working electrode connections of NRR process.

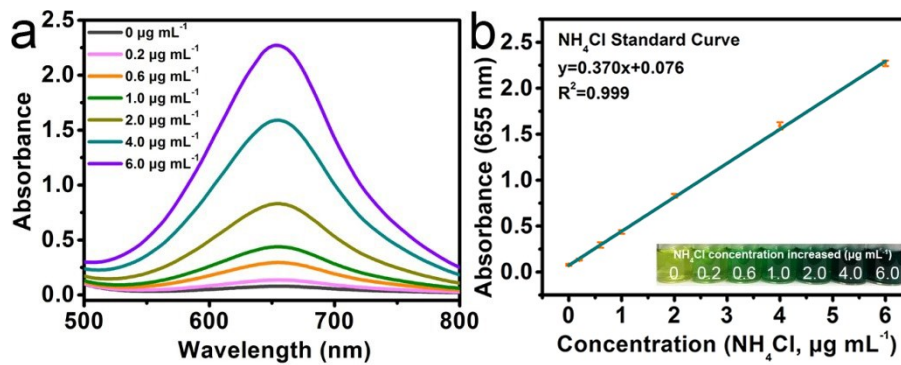


Fig. S2. (a) UV-Vis spectra of indophenol assays with NH_4Cl after incubated for 2 h at room temperature. (b) Calibration curve used for estimation of NH_4Cl .

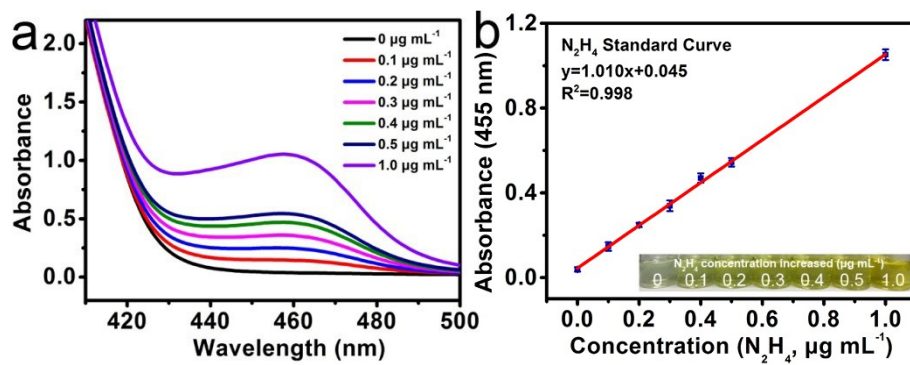


Fig. S3. (a) UV-Vis spectra of various N_2H_4 concentration after incubated for 20 min at room temperature. (b) Calibration curve used for calculation of N_2H_4 concentrations.

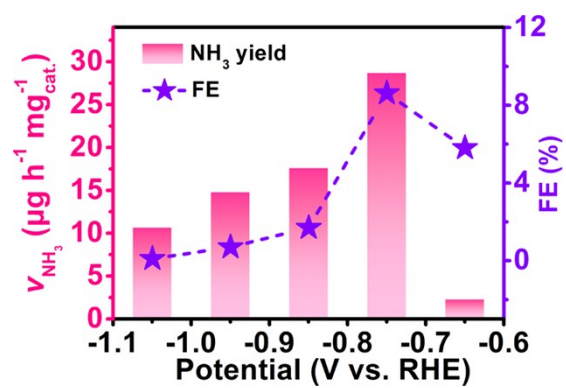


Fig. S4. NH_3 yields and FEs for $\text{Cr}_2\text{O}_3/\text{CPE}$ at a series of potentials for 2-h determined by ion chromatography analysis.

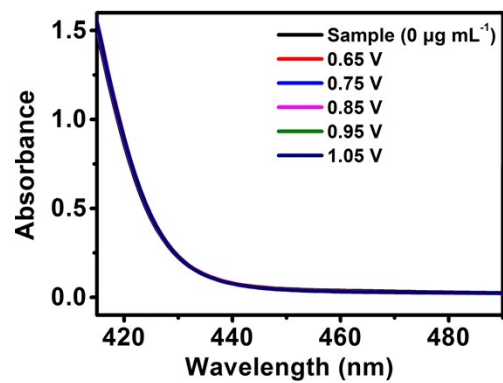


Fig. S5. UV-Vis spectra of the electrolyte estimated by the method of Watt and Chrisp before and after 2-h electrolysis in N₂ atmosphere at each given potential under ambient conditions.

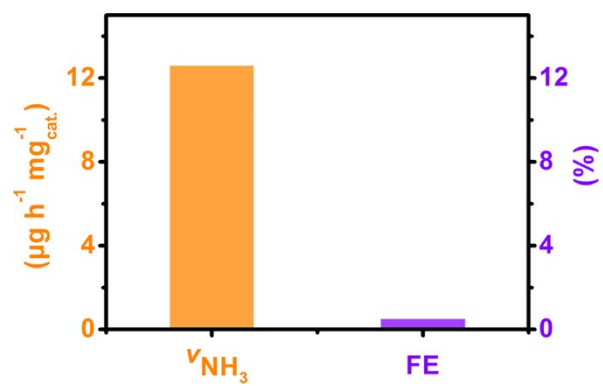


Fig. S6. NH_3 yield and FE for Ru/C at the potential of -0.75 V under ambient conditions in 0.1 M HCl.

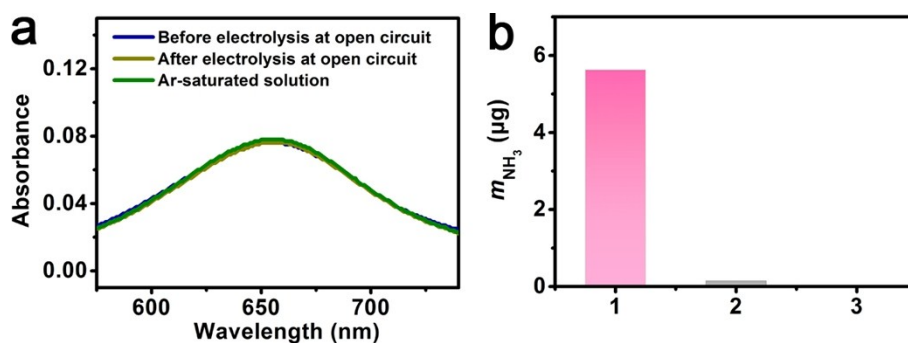


Fig. S7. (a) UV-Vis spectra of the electrolyte stained with indophenol indicator before and after 2-h electrolysis at open potential in N_2 -saturated solution and at the potential of -0.75 V in Ar-saturated solution on $\text{Cr}_2\text{O}_3/\text{CPE}$. (b) Production of NH_3 with $\text{Cr}_2\text{O}_3/\text{CPE}$ under different conditions: In N_2 -saturated solution and at the potential of -0.75 V (Column 1); In Ar-saturated solution and at the potential of -0.75 V (Column 2); In N_2 -saturated solution and at open potential (Column 3).

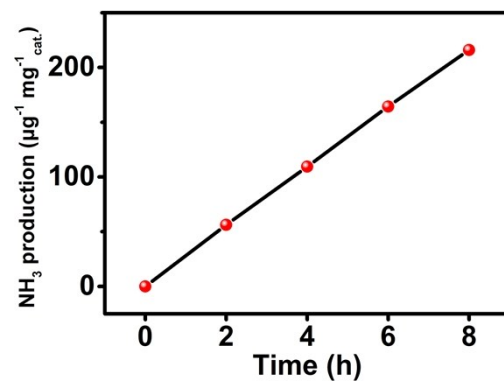


Fig. S8. The curve of NH₃ amount vs. reaction time at -0.75 V.

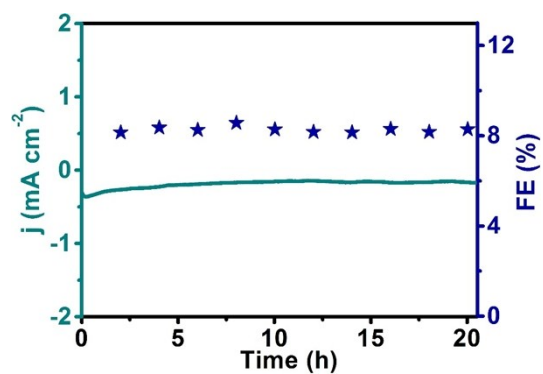


Fig. S9. Chronoamperometry and FE data for $\text{Cr}_2\text{O}_3/\text{CPE}$ at the potential of -0.75 V in N_2 -saturated 0.1 M HCl.

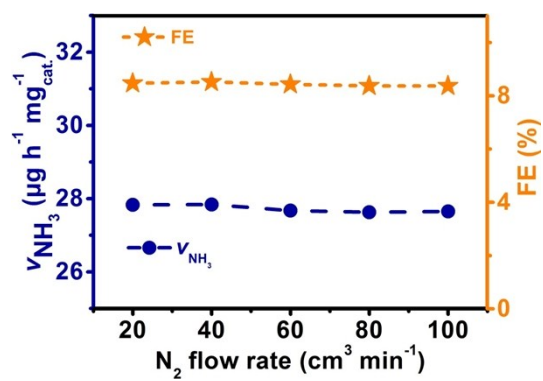


Fig. S10. NH₃ yield and FE for Cr₂O₃/CPE at the potential of -0.75 V with different N₂ flow rates.

Table S1. Comparison of the electrocatalytic N₂ reduction performance for Cr₂O₃ nanofiber with other NRR catalysts under ambient conditions.

Catalyst	Electrolyte	V_{NH_3}	FE	Ref.
Cr₂O₃/CPE	0.1 M HCl	28.13 $\mu\text{g h}^{-1} \text{mg}^{-1}_{\text{cat}}$	8.56%	This work
TA-reduced Au/TiO ₂	0.1 M HCl	21.40 $\mu\text{g h}^{-1} \text{mg}^{-1}_{\text{cat}}$	8.11%	[3]
α -Au/CeO _x -RGO	0.1 M HCl	8.31 $\mu\text{g h}^{-1} \text{mg}^{-1}_{\text{cat}}$	10.1%	[4]
Au nanorods	0.1 M KOH	6.04 $\mu\text{g h}^{-1} \text{mg}^{-1}_{\text{cat}}$	4%	[5]
AuHNCs	0.5 M LiClO ₄	3.90 $\mu\text{g h}^{-1} \text{cm}^{-2}$	30.2%	[6]
Ag-Au@ZIF	THF-based electrolyte	0.61 $\mu\text{g h}^{-1} \text{cm}^{-2}$	18%	[7]
Ru/Ti	0.5 M H ₂ SO ₄	7.34 $\mu\text{g h}^{-1} \text{cm}^{-2}$	-	[8]
Ru/C	2 M KOH	0.21 $\mu\text{g h}^{-1} \text{cm}^{-2}$	0.28%	[9]
Bi ₄ V ₂ O ₁₁ /CeO ₂	0.1 M HCl	23.21 $\mu\text{g h}^{-1} \text{mg}^{-1}_{\text{cat}}$	10.16%	[10]
MoO ₃	0.1 M HCl	29.43 $\mu\text{g h}^{-1} \text{mg}^{-1}$	1.9%	[11]
Mo ₂ N	0.1 M HCl	78.4 $\mu\text{g h}^{-1} \text{mg}^{-1}_{\text{cat}}$	4.5%	[12]
MoN	0.1 M HCl	0.06 $\mu\text{g h}^{-1} \text{cm}^{-2}$	1.15%	[13]
MoS ₂ /CC	0.1 M Na ₂ SO ₄	0.02 $\mu\text{g h}^{-1} \text{cm}^{-2}$	1.17%	[14]
Mo nanofilm	0.01 M H ₂ SO ₄	1.89 $\mu\text{g h}^{-1} \text{cm}^{-2}$	0.72%	[15]
PEBCD/C	0.5 M Li ₂ SO ₄	1.58 $\mu\text{g h}^{-1} \text{cm}^{-2}$	2.85%	[16]
Fe ₂ O ₃ -CNT	KHCO ₃	0.22 $\mu\text{g h}^{-1} \text{cm}^{-2}$	0.15%	[17]
Fe ₃ O ₄ /Ti	0.1 M Na ₂ SO ₄	0.012 $\mu\text{g h}^{-1} \text{cm}^{-2}$	2.6%	[18]
N-doped nanocarbon	0.05 M H ₂ SO ₄	27.20 $\mu\text{g h}^{-1} \text{mg}^{-1}_{\text{cat}}$	1.42%	[19]
B ₄ C	0.1 M HCl	26.57 $\mu\text{g h}^{-1} \text{mg}^{-1}_{\text{cat}}$	15.95%	[20]
Au flowers	0.1 M HCl	25.57 $\mu\text{g h}^{-1} \text{mg}^{-1}_{\text{cat}}$	6.05%	[21]
Ag nanosheet	0.1 M HCl	4.62 $\times 10^{-11} \text{mol s}^{-1} \text{cm}^{-2}$	4.8%	[22]

β -FeOOH nanorods	0.5 M LiClO ₄	23.32 $\mu\text{g h}^{-1} \text{mg}^{-1}_{\text{cat.}}$	6.7%	[23]
TiO ₂ -rGO	0.1 M Na ₂ SO ₄	15.13 $\mu\text{g h}^{-1} \text{mg}^{-1}_{\text{cat.}}$	3.3%	[24]

Table S2. Data obtained from the ion chromatography for NH_4^+ concentrations after electrolysis for 2-h at a series of potentials.

Potential	Concentration (NH_4^+, ppm)
-0.65 V	0.013
-0.75 V	0.164
-0.85 V	0.101
-0.95 V	0.085
-1.05 V	0.061

References

- [1] D. Zhu, L. Zhang, R. E. Ruther and R. J. Hamers, *Nat. Mater.*, 2013, **12**, 836–841.
- [2] G. W. Watt and J. D. Chrisp, *Anal. Chem.*, 1952, **24**, 2006–2008.
- [3] M. Shi, D. Bao, B. Wulan, Y. Li, Y. Zhang, J. Yan and Q. Jiang, *Adv. Mater.*, 2017, **29**, 1606550.
- [4] S. Li, D. Bao, M. Shi, B. Wulan, J. Yan and Q. Jiang, *Adv. Mater.*, 2017, **29**, 1700001.
- [5] D. Bao, Q. Zhang, F. Meng, H. Zhong, M. Shi, Y. Zhang, J. Yan, Q. Jiang and X. Zhang, *Adv. Mater.*, 2017, **29**, 1604799.
- [6] M. Nazemi, S. R. Panikkanval and M. A. El-Sayed, *Nano Energy*, 2018, **49**, 316–323.
- [7] H. K. Lee, C. S. L. Koh, Y. H. Lee, C. Liu, I. Y. Phang, X. Han, C. K. Tsung, X. Ling, *Sci. Adv.*, 2018, **4**, eaar3208.
- [8] K. Kugler, M. Luhn, J. A. Schramm, K. Rahimi and M. Wessling, *Phys. Chem. Chem. Phys.*, 2015, **17**, 3768–3782.
- [9] V. Kordali, G. Kyriacou and C. Lambrou, *Chem. Commun.*, 2000, **17**, 1673–1674.
- [10] C. Lv, C. Yan, G. Chen, Y. Ding, J. Sun, Y. Zhou and G. Yu, *Angew. Chem. Int. Ed.*, 2018, **57**, 6073–6076.
- [11] J. Han, X. Ji, X. Ren, G. Cui, L. Li, F. Xie, H. Wang, B. Li and X. Sun, *J. Mater. Chem. A*, 2018, **6**, 12974–12977.
- [12] X. Ren, G. Cui, L. Chen, F. Xie, Q. Wei, Z. Tian and X. Sun, *Chem. Commun.*, 2018, **54**, 8474–8477.
- [13] L. Zhang, X. Ji, X. Ren, Y. Luo, X. Shi, A. M. Asiri, B. Zheng and X. Sun, *ACS Sustainable Chem. Eng.*, 2018, **6**, 9550–9554.
- [14] L. Zhang, X. Ji, X. Ren, Y. Ma, X. Shi, Z. Tian, A. M. Asiri, L. Chen, B. Tang and X. Sun, *Adv. Mater.*, 2018, **30**, 1800191.
- [15] D. Yang, T. Chen and Z. Wang, *J. Mater. Chem. A*, 2017, **5**, 18967–18971.

- [16] G. Chen, X. Cao, S. Wu, X. Zeng, L. Ding, M. Zhu, H. Wang, *J. Am. Chem. Soc.*, 2017, **139**, 9771–9774.
- [17] S. Chen, S. Perathoner, C. Ampelli, C. Mebrahtu, D. Su, G. Centi, *Angew. Chem. Int. Ed.*, 2017, **56**, 2699–2703.
- [18] Q. Liu, X. Zhang, B. Zhang, Y. Luo, G. Cui, F. Xie and X. Sun, *Nanoscale*, 2018, **10**, 14386–14389.
- [19] Y. Liu, Y. Su, X. Quan, X. Fan, S. Chen, H. Yu, H. Zhao, Y. Zhang and J. Zhao, *ACS Catal.*, 2018, **8**, 1186–1191.
- [20] W. Qiu, X. Xie, J. Qiu, W. Fang, R. Liang, X. Ren, X. Ji, G. Cui, A. M. Asiri, G. Cui, Bo Tang and X. Sun, *Nat. Commun.*, 2018, **9**, 3485.
- [21] Z. Wang, Y. Li, H. Yu, Y. Xu, H. Xue, X. Li, H. Wang and L. Wang, *ChemSusChem*, 2018, DOI: 10.1002/cssc.201801444.
- [22] H. Huang, L. Xia, X. Shi, A. M. Asiri and X. Sun, *Chem. Commun.*, 2018, DOI: 10.1039/C8CC06365F.
- [23] X. Zhu, Z. Liu, Q. Liu, Y. Luo, X. Shi, A. M. Asiri, Y. Wu and X. Sun, *Chem. Commun.*, 2018, DOI: 10.1039/C8CC06366D.
- [24] X. Zhang, Q. Liu, X. Shi, A. M. Asiri, Y. Luo, X. Sun and T. Li, *J. Mater. Chem. A*, 2018, **6**, 17303–17306.